Egypt. J. Bot. **Vol. 63**, No. 3, pp. 1155-1171 (2023)

Egyptian Journal of Botany
http://ejbo.journals.ekb.eg/

In vitro Assessment of *Ulva lactuca* Mediated Selenium Nanoparticles (USeNPs) through Elevating the Action of Ketoconazole Antibiotic against Pathogenic Yeast Species and Wound Healing Capacity through Inhibition of Cyclooxygenase (Cox-1) Activity

Mofida E.M. Makhlof[(1)], Mostafa M. El-Sheekh[(2)#], Majdah M. Al-Tuwaijri[(3)], Khaled A. El-Tarabily[(4)], Abeer I.M. EL-Sayed[(1)]

[(1)]Department of Botany and Microbiology, Faculty of Science, Damanhour University, Damanhour, 22516, Egypt; [(2)]Botany Department, Faculty of Science, Tanta University, Tanta, 31527, Egypt; [(3)]Department of Biology, Faculty of Applied Science, Umm Al-Qura University, Makkah Al-Mukarramah, 21955, Saudi Arabia; [(4)]Department of Biology, College of Science, United Arab Emirates University, Al Ain, 15551, United Arab Emirates.

ULVA selenium nanoparticles (USeNPs) were synthesized and characterized, then examined for their wound healing capacity through *in vitro* assay showing promising healing (82.27%) with USeNPs concentration (500µg/mL). We also determined the antifungal potential via agar well diffusion technique, minimum inhibitory concentration (MIC), which was evaluated by a micro-dilution assay. The synergistic effect of the USeNPs individually or in combination with standard antifungal antibiotic (ketoconazole;100µg/mL) was studied against *Cryptococcus neoformans* RCMB 0049001 and *Candida lipolytica* RCMB 005007(1). *Geotrichum candidum* RCMB 041001 was also checked by agar well diffusion assay, followed by transmission electron microscopy to assess different changes in the most sensitive fungal yeast cells. The results indicated that USeNPs have a promising antifungal effect against *C. neoformans* RCMB 0049001 and *C. lipolytica* RCMB 005007(1) by achieving remarkable inhibition zones. In comparison, no effect was detected on *G. candidum* RCMB 041001. The MIC was found to be 78.1µg and 312.5µg for *C. neoformans* RCMB 0049001 and *C. lipolytica* RCMB 005007(1), respectively. The biosynthetic USeNPs have a strong antifungal potential and can elevate and strengthen the action of ketoconazole antibiotic towards different fungal pathogens, and this was obvious In the experiment of synergism carried out in the present study based on combining ketoconazole;100µg/mL with USeNPs, which resulted in a detached *C. neoformas* RCMB 0049001 cells with a severe dramatic change.

Keywords: *Candida lipolytica*, *Cryptococcus neoformas,* Cyclooxygenase (Cox-1), Ketoconazole, Wound healing, *Ulva lactuca, Ulva* selenium nanoparticles.

Introduction

Nanoparticles are of interest to scientists due to their high surface area and ability to interact effectively in numerous site reactions. Synthesizing nanoparticles involves a wide variety of approaches, including chemical, physical, and biological ones (Eldarier et al., 2020; Elsayed et al., 2022). The biological approach is the cleanest and safest of all the procedures (Chugh et al., 2021). The green trend of nanoparticles synthesis is a self-sustaining, secure, eco-friendly, and relatively low-cost alternative to standard nanoparticles manufacturing methods (Youssef et al., 2019; Jain, 2022).

The biological approach has beneficial characteristics such as the absence of hazardous compounds such as stabilizers or reductants, the absence of harmful returns, low energy consumption, and the capacity to produce on a

#Corresponding author email: mostafaelsheikh@science.tanta.edu.eg
Received 27/06/2023; Accepted 11/08/2023
DOI: 10.21608/ejbo.2023.220267.2393
Edited by: Prof. Salama A. Ouf, Faculty of Science, Cairo University, Giza 12613, Egypt.

large scale, making green synthesis methods more appealing and preferred (Jain, 2022). Because of their high biosafety and effectiveness in creating nanoparticles with attractive bioactive characteristics, the use of algal biomass/extracts as precursors in nanoparticles synthesis is becoming increasingly prevalent (Hifney et al., 2022; Makhlof et al., 2022; Touliabah et al., 2022; Abo-Neima et al., 2023). However, the algal macromolecules involved in metal nanoparticle biosynthesis are underutilized in comparison to other comparable sources such as plants or microorganisms (Jacob et al., 2021).

Secondary metabolites from algae have been demonstrated to reduce metal precursors to nanoparticles; additionally, the natural components of algae act as capping and stabilizing agents in the conversion of metal compounds to metal, metal oxides, or bimetallic nanoparticles (Jain, 2022; Sampath et al., 2022). Phycosynthesized nanoparticles have already been evaluated for anti-cancer, anti-fouling, anti-microbial, and bioremediation activities (El-Sheekh et al., 2021; Jain, 2022; Abo-Neima et al., 2023).

Wound healing is a novel application of biogenic selenium nanoparticles, as nanoparticles are a significant agent for treating and preventing wound consequences, with various advantages over standard-of-care (SOC) treatments (Naskar & Kim, 2020). Nanoparticles have a diameter of 1-100nm and are being studied extensively in the biomedical and tissue engineering fields. There are two different healing techniques for wounds, nanoparticles with real wound healing properties and nanoparticles as drug delivery systems. Their main characteristics include controlled and continuous spread, enhanced medication half-life, and bioavailability (Verma & Kumar, 2022). Shalaby et al. (2022) demonstrated that nanoparticles are the key to a new era in biocompatible drug delivery. According to Toczek et al. (2022), many types of wounds are difficult to control surgically using standard therapies; nevertheless, if silver, as well as gold and its corresponding nanoparticles, improve wound healing, they should be used immediately in contemporary gynecological practice (Shalaby et al., 2022).

Current chronic wound therapies are intended to cover the wound, prevent pathogen infection, remove dead tissue, moisturize the wound, and suck excess secretions (Blanco-Fernandez et al., 2021). The *in vitro* scratch assay is a straightforward, low-cost, and well-established method for evaluating cell migration *in vitro* (Todaro et al., 1965). *In vitro* scratch assays are well suited for research on the impact of cell migration by cell-matrix and cell-cell interactions, simulating *in vivo* wound healing cell migration, and are suitable for image analysis of live cells during migration to observe intracellular events if necessary (Haudenschild & Schwartz, 1979). This method has been used to examine the migration of individual cells at the scratch's leading edge as well as to track the migration of homogeneous cell populations (Haudenschild & Schwartz, 1979).

There is a diversity of organisms in the marine habitat, such as algae (green, brown, and red), which should be investigated and their chemical composition assessed (Amin, 2020). *Ulva lactuca* is a type of green macroalga known as green sea lettuce or green laver. *U. lactuca's* chemical composition contains proteins, phenolic compounds, carbohydrates, carotenoids, flavonoids, alkaloids, terpenes, and other biomolecules, allowing it to be used as a green option for manufacturing nanoparticles (Amin, 2019).

Because of societal and environmental changes, population ageing, and an increase in vulnerable persons (such as patients with predisposing factors), the prevalence of superficial mycosis has increased in recent years, generating global health consequences (Rónavári et al., 2018; El Maghraby & Hassan, 2021). Dermatomycosis usually manifests as an allergic, painful tinea on the toes, inner thighs, causing the affected area to peel and blister. Hair loss and thicker or malformed fingernails can result from fungi that spread to the scalp or nails. Dermatomycosis is primarily caused by filamentous dermatophytes such as *Microsporum* spp., *Trichophyton* spp., or *Epidermophyton* spp.; however, keratinized tissues can be penetrated by exploitative yeast species such as *Candida* or *Cryptococcus*. Because the causal microorganisms (*Candida* spp.) are either permanent or transitory components of the human skin microflora, cutaneous candidiasis is an endogenous process. Systemic mycoses caused by fungi have become a severe concern as well as a clinical and pharmaceutical issue since the turn of the century, particularly for people with immunological deficiencies (Perfect, 2013). Glucocorticoid medication, immunotherapy, oncological and haematological disorders, increasing transplants, surgical operations, and patients with acquired immunodeficiency syndrome (AIDS) are all connected to an increase in fungal

infections, along with other variables (Liao et al., 2016).

Among eukaryotes, the basidiomycete *Cryptococcus* spp., of which *Cryptococcus neoformans* is the type species, is unique in that it is a haploid, spherical yeast enclosed in a polysaccharide (PS) capsule (McFadden et al., 2006). *Cryptococcus* spp., found worldwide, is responsible for around 181,100 deaths each year (Rajasingham et al., 2017). The host becomes infected after inhaling spores or dehydrated yeasts. The infection can either be latent, with no clinical symptoms, or manifest as an acute version of the disease. Because *Cryptococcus* spp. prefers to colonize the central nervous system (CNS) and can do so through a multitude of concurrent infection paths; cryptococcal meningitis may be regarded as the most dangerous case of cryptococcosis (WHO, 2018; Araújo et al., 2021).

Regardless of the etiology of *Cryptococcus neoformans* infection, this organism can cause serious injury to the host. Finding innovative and effective treatments for opportunistic infections and species that cause cutaneous mycosis is thus a pressing medical need. An innovative, eco-friendly, and cost-effective method is required to achieve this goal. Because of the numerous recent scientific advancements in this field, a solution that meets these requirements might be built on nanotechnology because we can now build nanoparticles with diverse properties suitable for specific applications (Rónavári et al., 2018).

According to Ellis & Watson (1996), ketoconazole is an oral or topical synthetic dioxolane imidazole molecule that inhibits ergosterol formation, producing alterations in specific cell membrane activities, with strong homology to keratin and a wide range of action, including dermatophytes and yeasts. On the other hand, ketoconazole has emerged as the medicine of choice for treating Malassezia infections and is a critical adjuvant in treating AIDS patients with fluconazole-resistant *Candida* infections. After topical treatment, ketoconazole is not systemically absorbed; however, it is efficiently taken orally under acidic conditions. The most common adverse effects seen in patients treated with this antibiotic are nausea, anorexia, and vomiting, which occur in about 20% of cases, and the metabolism of adrenal or testicular steroid hormones may be altered (Ellis & Watson, 1996).

The current research aims to look at the use of *Ulva lactuca* mediated selenium nanoparticles (USeNPs) in the manufacture of wound dressings. Gold, silver, copper, cuprous, and zinc oxide are the most commonly utilized biosynthesized nanoparticles (Jain, 2022). So, in the current study, USeNPs will be used for the first time in wound healing treatment, with the anti-inflammatory activity and potential to boost ketoconazole antifungal action via loading this drug over our USeNPs being evaluated.

Materials and Methods

Biosynthesis and characterization of USeNPs

Ulva lactuca was collected from the Gulf of Suez, Egypt. Tap water was used to rinse the samples to remove salt, biota, debris, and sand. Drying was accomplished through shade air drying, followed by 3h of oven drying at 60°C. Dried *U. lactuca* was ground in a grinder (Brown mill), and 10g of *U. lactuca* powder was mixed, stirred, and boiled with 100mL of deionized water for 30min. One mM Na_2SeO_4 (Sigma-Aldrich, Inc., St. Louis, MO, USA) reduction was made using *U. lactuca* aqueous extract with a ratio (1:9) alga extract: Na_2SeO_4 solution.

The observed red color of USeNPs after 3 days at room temperature with dark stirring was validated by a UV-Vis spectrophotometer (Thermo Scientific Evolution TM 300, Thermo Fisher Scientific, Waltham, MA, USA) at a wavelength range of 200 to 800nm, and the solution was centrifuged at 10,000 rpm for 30min. USeNPs were then washed using double distilled water, followed by pure ethanol, then dried at 50°C within the airtight container and were kept for further characterization and application.

For USeNPs shape and size detection, transmission electron microscopy (TEM) (JEM-2100, JEOL, Ltd., Tokyo, Japan) and scanning electron microscopy (SEM) (JSM 6490 LV, JEOL, Ltd., Tokyo, Japan) were used. An energy dispersive X-ray (EDX) study for USeNPs was carried out between 0 and 12keV. XRD-6000 detector (Shimadzu Corp., Kyoto, Japan) was used for USeNPs elementary and crystallinity confirmation at 30kV and 10 mA with 2.2 KW Cu anode radiation.

Functional groups responsible for selenium ions' reduction and capping were identified under

the range of 400–4000cm^{-1} using Fourier transform infrared **(**FTIR) spectroscopy, while the effective surface charges of USeNPs at various variables and the long-term of its stability were estimated using a Zeta analyzer (ZetaPlus, Brookhaven Instruments, Holtsville, NY, USA) as Zeta potential between - 20 and + 20mV.

Cytotoxicity of USeNPS with WISH cells

WISH cell line (human amnion epithelial) was supplied from the ATCC, Manassas, VA, USA, and has been used for toxicity analysis of USeNPs using MTT assay. Such cell line type was used due to its higher stability compared with other primary amnion cells' cultures (Kumar et al., 2004). RPMI 1640 was chosen for cell line growth, adding antimycotic solution (100×1mL/100mL of medium) in a humid atmosphere of 5% carbon dioxide at 37**°**C.

Cell viability detection by the dye trypan blue was used for each cell batch as an exclusion test before the experiments. The batches that exhibited more than 95% cell viability and passage number from 10 to 15 for the cytotoxicity test were used. Different concentrations (31.25, 62.5, 125, 250, 500, and 1000) µg/mL of USeNPs were then seeded in 96-well plates with (1 × 10^4/100µL/well) cells concentration using a complete RPMI medium for 24h at 37**°**C (Saquib et al., 2012).

Evaluation of wound healing ability of USeNPs by in vitro scratch assay

We created a "scratch" in one layer of cells, then photographed it at the start and end of a defined period to show cell migration scratch closure, and the photos were compared to show the healing percent (Liang et al., 2007).

Fibroblasts extracellular matrix (ECM) of 10mg/mL fibronectin or 50mg/mL poly-L-lysine as a control was applied to cover dishes 60 mm in size, then incubated at 4°C overnight or 37°C for 2h without shaking. The unbound ECM substrate was discarded, and the coated plates were blocked for 1h at 37°C with 3mL bovine serum albumin at concertation 2mg/mL. The dishes were then washed with phosphate-buffered saline (PBS) before being refilled with 3-5mL of Dulbecco's modified Eagle's medium, which included certain supplements such as Versene (EDTA) with trypsin (serum, antibiotics) before cell plating.

Before adding the cells, the necessary concentration of USeNPs (500µg/mL) was added to the media, and the developing cells were suspended in a tissue culture dish using PBS as a wash two times, then versene containing trypsin was added, and the cells were combined with the serum-containing solution. The solution was carefully absorbed with a pipette, and the dish was struck to ensure the cells were evenly distributed.

Cell count was determined using a hemocytometer, then the cells were seeded in the previously prepared 60-mm dish to generate the appropriate monolayer, and the cells were incubated for approximately 6h at 37°C to allow complete adherence and dissemination of cells in the substrate. Then, using p200 pipet tips, we created a ''scratch'' of identical size in both the control and USeNPs treatments, eliminating cell debris and smoothing the scratch edge by one-time cell washing with 1mL growth solution and then replacing it with 5mL of liquid. For both control and USeNPS-treated cells, images were captured using a phase-contrast microscope at the zero-time picture and after incubation for 8-18h at 37°C.

We conducted quantitative analysis on the photos using Pro-Plus software (Media Cybernetics) or freeware (http://rsb.info.nih.gov/ij/) by calculating the distances between the sides of the scratch in millimeters (Liang et al., 2007).

In vitro cyclooxygenase (Cox-1) inhibition assay

USeNPs inhibition ability over Cox-1 isoenzymes was estimated using (catalog number k548, Biovision, USA) kit according to the manufacturer's instructions. USeNPs with the desired concentrations ranging from 0.25 – 500µg/mL were prepared using 1.0% DMSO as a solvent in 1mL final volume with the use of indomethacin as a positive control for the Cox-1 inhibition assay and with the calculation of USeNPs IC_{50} (the concentration that causes 50% inhibition) from the curve of concentration-response using GraphPad PRISM (Abdel-Aziz et al., 2016).

Evaluation of antifungal activity

Because of the significant infections produced by them, as well as the fact that they are antibiotic-resistant pathogens, three yeast strains were chosen to investigate the effect of the USeNPs: *Cryptococcus neoformas* RCMB 0049001, *Candida lipolytica* RCMB 005007(1), and *Geotrichum candidum* RCMB 041001.

The agar well diffusion technique was utilized to detect the effect of USeNPs, while ketoconazole (100µg/mL) served as an antifungal activity

standard. For antifungal activity, Sabouraud Dextrose Agar (SDA) was used for the maintenance of tested pathogenic fungal species (*C. neoformas* RCMB 0049001, *C. lipolytica* RCMB 005007(1) and *G. candidum* RCMB 041001). Aliquots (100µL) of pathogenic yeast culture broth (CFU $3x10^3$ cells/mL) were dispersed into Petri plates using sterile glass spreaders, and two 6mm diameter wells were created with a sterilized cork borer.

One well was loaded with 100µL of ketoconazole (100µg/mL), and the second well was loaded with 100µL of USeNPS alone (2.5mg/mL). The cells were then incubated for 5 days at 28°C. The inhibition zones were checked and measured in millimeters using a transparent ruler. The data were presented as mean, standard deviation (SD), and the experiment was repeated three times (Abdel-Moneim et al., 2022).

Determination of the minimum inhibitory concentration (MIC)

The MIC of USeNPs with standard antifungal ketoconazole (100µg/mL) was determined using an Ericsson & Sherris (1971) micro-dilution assay. Aliquots (100µL) of USeNPs at various concentrations were homogenized in Sabouraud dextrose broth (SDB) tubes that had already been inoculated with 100µL fungal spore suspension size (3×10^3 CFU/mL). The untreated control was inoculated with only *C. neoformas* RCMB 0049001 and *C. lipolytica* RCMB 005007(1). All tubes were incubated for 5 days at 28°C. The MIC was calculated as the lowest antifungal agent (USeNPs) concentration that stopped fungal growth (EL-Saadony et al., 2021).

Synergistic antifungal activity of USeNPs with ketoconazole

The agar well diffusion experiment was used to evaluate the synergistic effect of USeNPs with antifungal antibiotic (ketoconazole (100µg/mL) in inhibiting the development of *C. neoformas* RCMB 0049001 and *C. lipolytica* RCMB 005007(1).

SDA plates were inoculated with 100µL of activated cultures of the two pathogenic fungi, and five wells were created in each plate. The first well was filled with 100µL ketoconazole (100µg/mL) +2.5mg/mL USeNPs, the second well with 100µL (100µg/mL) ketoconazole +5mg/mL USeNPs, the third well with 100µL ketoconazole as a control, the fourth well with 2.5mg/mL USeNPs only, and the fifth well with 5mg/mL USeNPs only. Incubation was done at 28°C for 5 days.

The transparent ruler was used to measure the inhibitory zone diameters surrounding the wells (stated in mm) to assess synergistic antifungal effects. The data were presented as mean, standard deviation (SD), and the experiment was repeated three times (Aabed & Mohammed, 2021).

TEM

TEM was used to show the differences in pathogenic *C. neoformas* RCMB 0049001 cells before and after treatment with 5mg/mL USeNPs alone and combined with the antibiotic ketoconazole (100µg/mL). After being centrifuged at 4000 rpm for 10min to remove debris from a 5-day-old fungal culture, the cells were washed in distilled water, fixed in 3% glutaraldehyde for 5min at room temperature, rinsed, and post-fixed in phosphate buffer and potassium permanganate solution. The samples were then dehydrated using ethanol concentrations ranging from 10% to 90% for 15min in each alcohol dilution and finally with absolute ethanol for 30min. Finally, the samples were infiltrated using epoxy resin and acetone in a graded series until they were finally in pure resin.

Thin slices were mounted on copper grids for examination. At Al-Azhar University's Regional Center for Mycology and Biotechnology (RCMB), sections were double-stained with uranyl acetate, then with lead citrate, and finally examined with a JEOL - JEM 1010 TEM at 70 kV (Amin, 2016; Amin et al., 2020; Amin et al., 2022).

Statistical analyses

There were three separate runs for each experiment. Using the descriptive statistics frequencies in Statistical Package for Microsoft Excel, the findings were reported as the mean SD.

Results

Characterization of USeNPs

USeNPs were characterized using the following techniques, UV–Vis spectra, TEM, SEM, FTIR, EDX, X-ray diffraction (XRD), and Zeta potential. The zeta potential was negative with a value of −19.0 ± 6.17mV and polydispersity index value (PDI = 0.405), and USeNPs recorded the highest peak at wavelength 610. Figure 1a &b shows the TEM images of USeNPs with a smooth spherical shape and 46.03-83.80nm size.

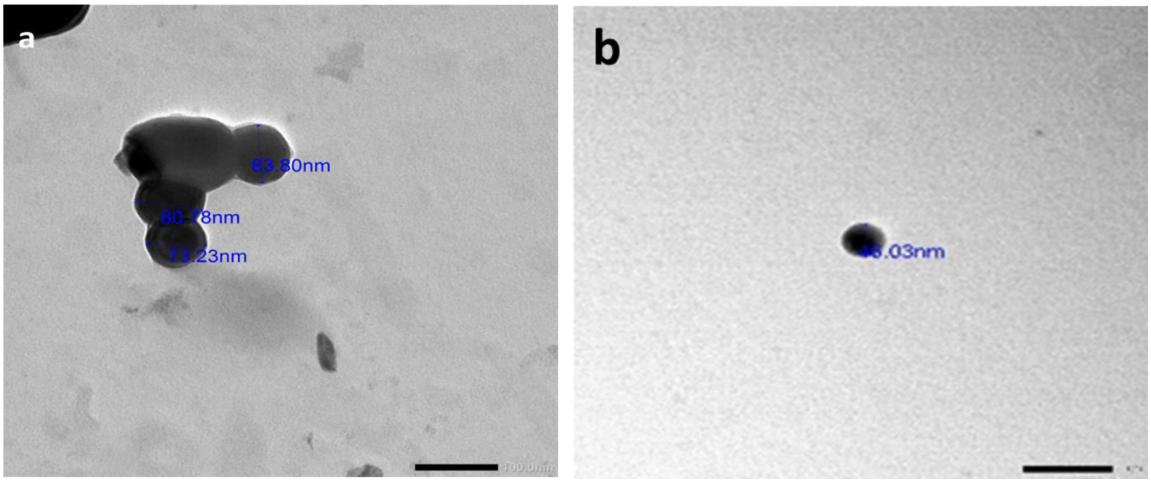

Fig. 1. Transmission electron microscopy (TEM) images (a, and b) of the *Ulva lactuca* mediated selenium nanoparticles (USeNPs) (100nm), showing different particle size

Figure 2 displays the SEM of the phycosynthesized USeNPs, which demonstrated that the nanoparticles were oval, spherical, and had a particle size of roughly 24.32 - 27.53nm. The elemental analysis (Figs. 3, 4) via EDX analysis showed a selenium signal along with carbon and oxygen group peaks. The presence of selenium was confirmed in the sample with 8.31%. The examination also revealed carbon (43.96%) and oxygen (29.95%) signals.

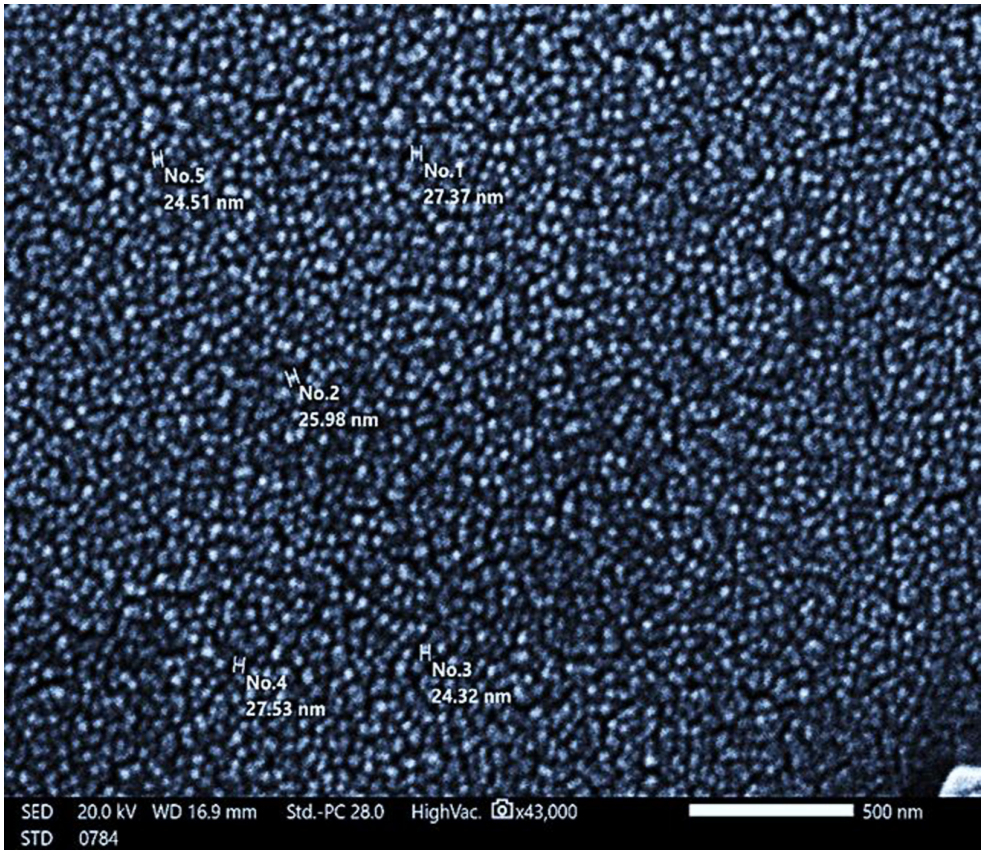

Fig. 2. Scanning electron microscopy (SEM) images of *Ulva lactuca* mediated selenium nanoparticles (USeNPs) (500nm), with different particles size

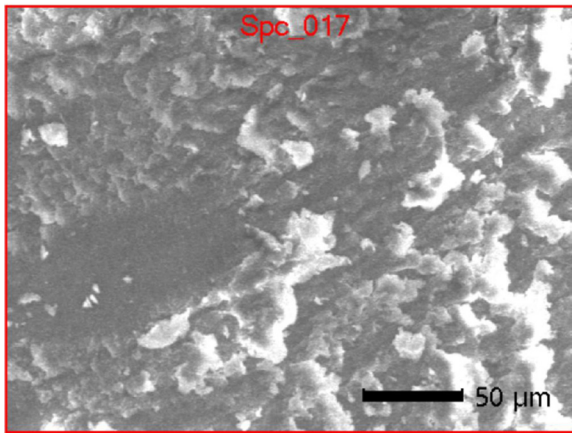

Fig. 3. Field of energy dispersive X-ray (EDX) analysis of *Ulva lactuca* mediated selenium nanoparticles (USeNPs)

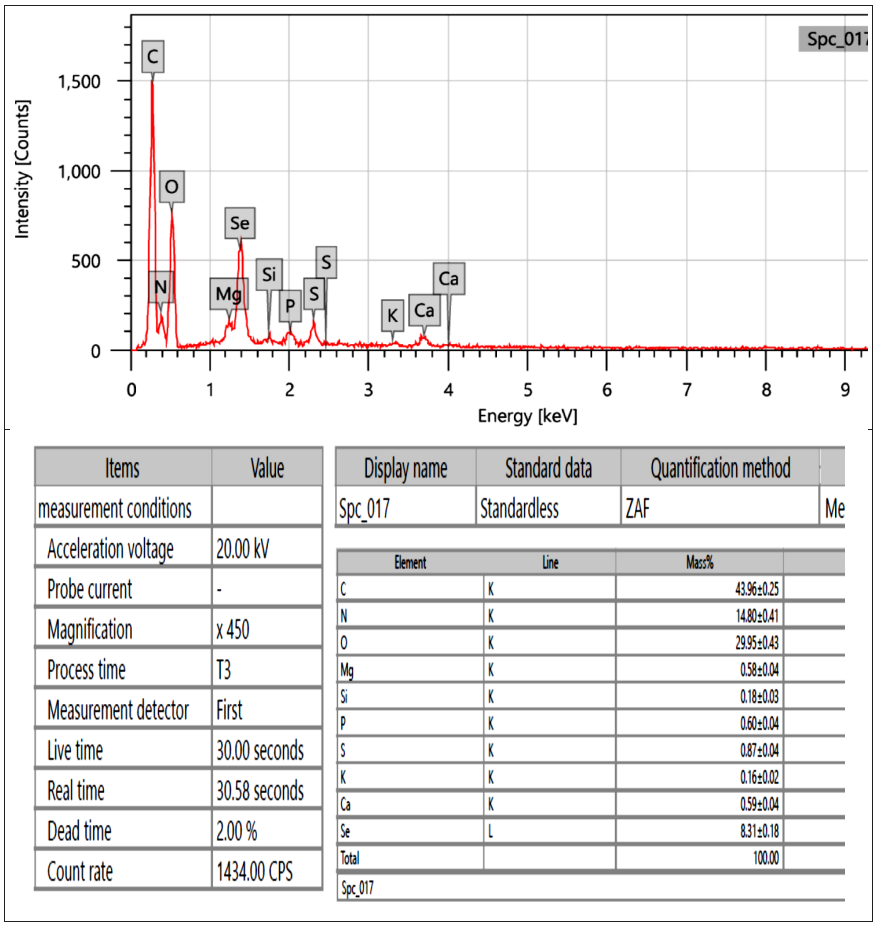

Items	Value
measurement conditions	
Acceleration voltage	20.00 kV
Probe current	-
Magnification	x 450
Process time	T3
Measurement detector	First
Live time	30.00 seconds
Real time	30.58 seconds
Dead time	2.00 %
Count rate	1434.00 CPS

Display name	Standard data	Quantification method	
Spc_017	Standardless	ZAF	Me

Element	Line	Mass%
C	K	43.96±0.25
N	K	14.80±0.41
O	K	29.95±0.43
Mg	K	0.58±0.04
Si	K	0.18±0.03
P	K	0.60±0.04
S	K	0.87±0.04
K	K	0.16±0.02
Ca	K	0.59±0.04
Se	L	8.31±0.18
Total		100.00

Spc_017

Fig. 4. Analysis of the *Ulva lactuca* mediated selenium nanoparticles (USeNPs) EDX results

Evaluation of wound healing ability of USeNPs by in vitro scratch assay

Using a normal cell line (WISH cells), we conducted an *in vitro* scratching assay in order to evaluate the percentage of wound healing, as well as the change in wound width at zero time and after 24h (Figure 5A–C). The initial gap size was 2424003m, which decreased to 612700 and 429700 m after 24h, with 74.72 and 82.27% healing for control and USeNPs (500µg/mL) treated cells, respectively. WISH cells with an IC_{50} of 904.8µg/mL (Table 1) achieved 66% viability and 34% inhibition at the applied USeNPs dose (500µg/mL).

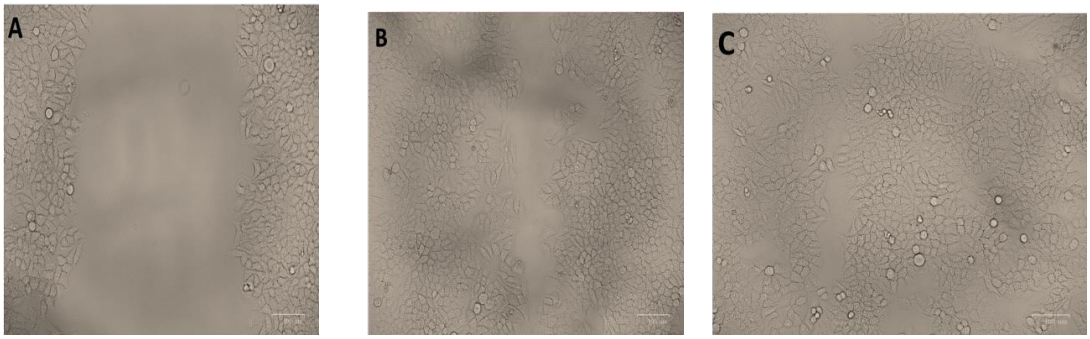

Fig. 5. Wound healing through cell migration A: the wound at 0h, B: the control wound after 24h, C: wound treated with *Ulva lactuca* mediated selenium nanoparticles (USeNPs (500µg/mL) after 24h

TABLE 1. Cytotoxicity of *Ulva lactuca* mediated selenium nanoparticles (USeNPs) with WISH cell line

Concentration of USeNPs (µg/mL)	OD_T	Viability (%)	Inhibition (%)
31.25	1.344	89	11
62.5	1.263	84	16
125	1.142	76	24
250	1.031	69	31
500	0.989	66	34
1000	0.66	44	56
OD_c		1.495	
IC_{50}		904.8	

ODT, optical density; IC_{50}, the half-maximal inhibitory concentration (IC_{50}) values (the concentration required for 50% inhibition of viability).

Inhibition of Cox-1 activity by USeNPs

Figure 6 displays the results of utilizing indomethacin as a standard to evaluate the inhibitory effect of UseNPs on the Cox-1 enzyme. The results showed that USeNPs inhibited Cox-1 activity in all concentrations except (0.25-0.5-1) µg/mL, with the maximum inhibition % 69.41 with IC50= 215.01µg/mL occurring at USeNPs concentration (500µg/mL) but did not reach the reference indomethacin.

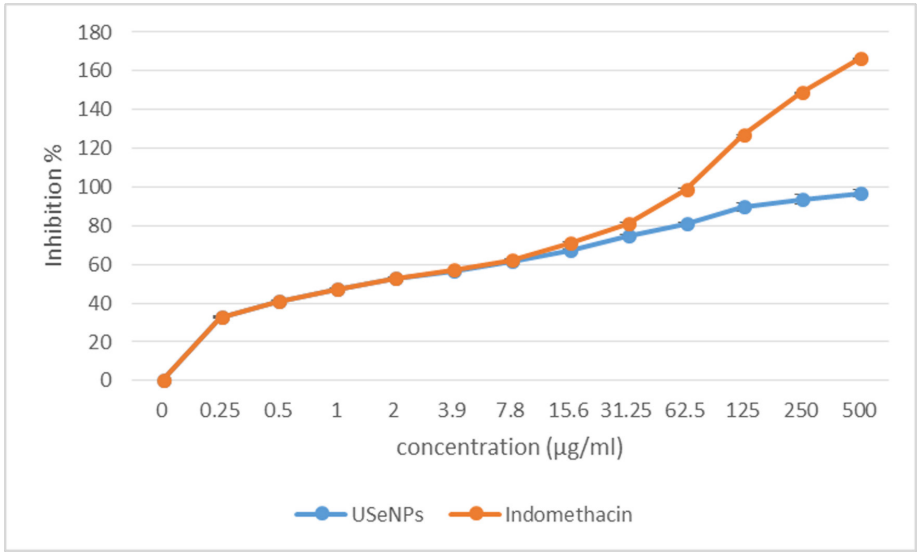

Fig. 6. Cox-1 inhibition (%) of *Ulva lactuca* mediated selenium nanoparticles (USeNPs) and indomethacin reference standard

Evaluation of antifungal activity

The phycosynthesized UseNPs demonstrated impressive antifungal activity against *C. neoformas* RCMB 0049001 and *C. lipolytica* RCMB 005007(1), with inhibition zones measuring 9.667 mm and 8.83 mm, respectively. However, *G. candidum* RCMB 041001 was unaffected. However, was the ketoconazole drug inhibited none of the studied fungal infections (Table 2).

MIC

Table 3 shows the MIC of USeNPs against the investigated fungal strains. Concentrations of 78.1µg/mL demonstrated promising suppression of *C. neoformas* RCMB 0049001, while 312.5µg/mL demonstrated considerable inhibition of *C. lipolytica* RCMB 005007(1). Compared to *C. lipolytica* RCMB 005007(1), the antifungal activity of the synthesized USeNPs was much more effective against *C. neoformas* RCMB 0049001 (Table 3).

Synergistic antifungal activity of USeNPs with ketoconazole

Table 4 shows that a treatment formula of 2.5mg/mL USeNPs combined with 100µg/mL ketoconazole can inhibit *C. neoformas* RCMB 0049001 and then *C. lipolytica* RCMB 005007(1), with inhibition zones of 12.833 and 10.173, respectively (Table 4).

The concentration of 5 mg/mL recorded a greater inhibition zone diameter against *C. neoformas* RCMB 0049001 followed by *C. lipolytica* RCMB 005007(1) (Table 4). Ketoconazole on its own was unable to inhibit the growth of fungi, but when it was combined with our USeNPs, the inhibition effect was amplified in a way that is readily apparent (Fig. 7).

TEM

The TEM micrographs of *C. neoformas* RCMB 0049001 treated with USeNPs individually and in combination with ketoconazole are shown in Fig. 8A-F. Individual *C. neoformas* RCMB 0049001 cells in the control sample were visible in micrographs (Fig. 8A, B), with only spherical or oval-cylindrical shaped conidia. In contrast, when *C. neoformas* RCMB 0049001 was treated with USeNPs, Fig. 8C, D shows yeast cells with abnormal morphology, some pores, and distorted membranes. The combination of USeNPs and the antifungal ketoconazole causes cell membrane disruption by creating abnormal surface bulges and a loss of smoothness in the membrane (Fig. 8E, F).

Discussion

In the present investigation, the surface charge of the USeNPs was detected using a zeta potential, which was found to be 19.0 ± 6.17mV. This zeta value indicates that USeNPs have high stability when forming a colloidal solution with water, as the negative charge on the surface of nanoparticles induces repulsion between them, resulting in nanoparticle stability (Mohamed et al., 2022). The current study's polydispersity index (PDI = 0.405) value indicates that USeNPs are polydispersed. This value is in the homogenous size distribution range (0-1), as when PDI > 1, the size distribution homogeneity drops and increases as the PDI approaches zero (Yedurkar et al., 2017).

TABLE 2. Antifungal activity of *Ulva lactuca* mediated selenium nanoparticles (USeNPs) against fungal pathogens

Pathogenic fungal strains	*Ulva lactuca* SeNPs (2.5mg/mL)	Ketoconazole as a control (100µg/mL)
Cryptococcus neoformas RCMB 0049001	9.667 ± 0.85	NA
Candida lipolytica RCMB 005007(1)	8.833 ± 0.62	NA
Geotrichum candidum RCMB 041001)	NA	NA

TABLE 3. Minimum inhibitory concentration (MIC) of *Ulva lactuca* mediated selenium nanoparticles (USeNPs) against fungal pathogens

Pathogenic fungal strains	MIC of USeNPs (µg/mL)	Ketoconazole as a control (100µg/mL)
Cryptococcus neoformas RCMB 0049001	78.1	NA
*Candida lipolytic*a RCMB 005007(1)	312.5	NA

TABLE 4. Synergistic antifungal activity of *Ulva lactuca* mediated selenium nanoparticles (USeNPs) individually and with ketoconazole

Pathogenic fungal strains	USeNPs (2.5mg/mL)	USeNPs (5mg/mL)	USeNPs (2.5mg/mL) + ketoconazole (100µg/mL)	USeNPs (5mg/mL) + ketoconazole (100µg/mL)	Ketoconazole as a control (100µg/mL)
Cryptococcus neoformas RCMB 0049001	9.66 ± 0.85	13.16 ± 0.62	12.83 ± 0.42	15.25 ± 0.70	NA
Candida lipolytica RCMB 005007(1)	8.83 ± 0.62	11.83 ± 0.62	10.17 ± 0.78	14.16 ± 0.62	NA
Geotrichum candidum RCMB 041001)	NA	NA	NA	NA	NA

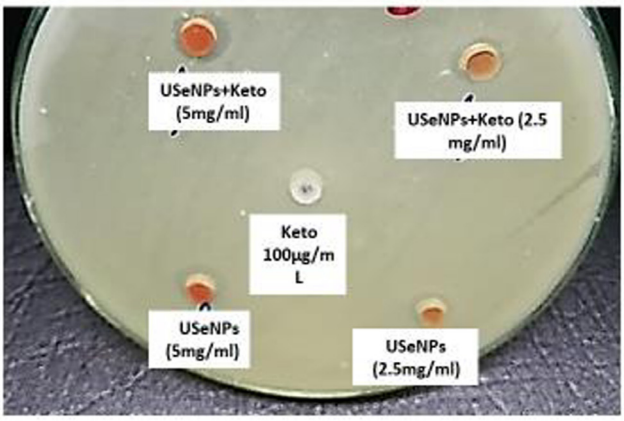

Fig. 7. Synergetic inhibition effect of *Cryptococcus neoformas* RCMB 0049001 by the action of *Ulva lactuca* mediated selenium nanoparticles (USeNPs) with ketoconazole; USeNPs (2.5mg/mL), USeNPs (5mg/mL), USeNPs (2.5mg/mL) + ketoconazole, USeNPs (5mg/mL) + ketoconazole, ketoconazole only (100µg/mL). Ketoconazole was used in concentration of 100µg/mL

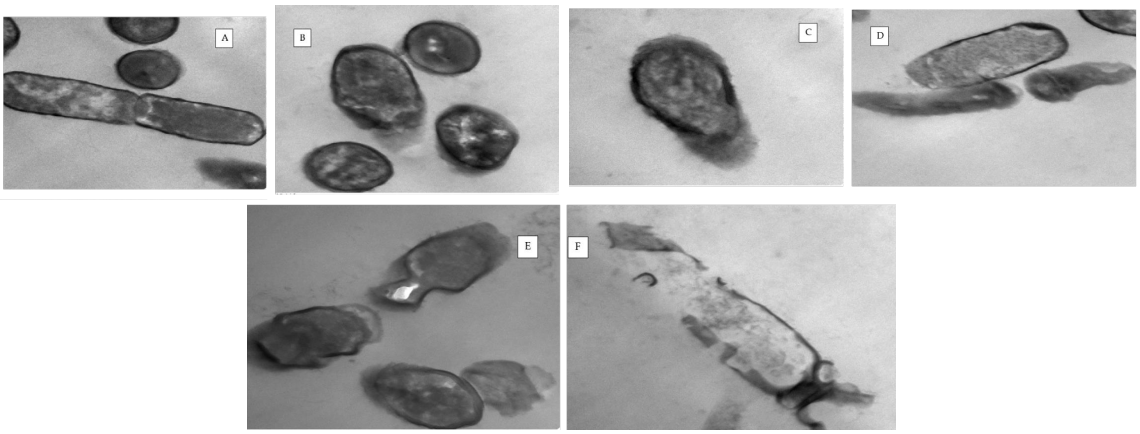

Fig. 8. Morphological alterations of *Cryptococcus neoformas* RCMB 0049001 yeast cells treated with *Ulva lactuca* mediated selenium nanoparticles (USeNPs) alone and in combination with ketoconazole (A and B) showing the untreated *Cryptococcus* cells with a compact cell wall, continuous cytoplasmic membrane, homogeneous and electron-dense cytoplasm and a polysaccharide capsule surrounding the cell. (C and D), yeasts treated with USeNPs alone had a disrupted cytoplasmic membrane cell wall and increased cell wall thickness. (E and F) the synergetic effect of USeNPs in combination with ketoconazole leads to the obvious destruction of membrane integrity, subsequently, the formation of pores and cell death of *Cryptococcus neoformans*

Furthermore, the phycosynthesized USeNPs have the largest absorption peak at wavelength 610, and the X-ray energy spectrum was used to confirm the elemental composition of USeNPs generated by *U. lactuca*. The peaks produced by XRD enhanced the synthesis of crystalline, spherical-shaped USeNPs. Furthermore, based on previous findings, the FTIR of blue-green algae had a high degree of similarity with only a slight deviation in the detected absorbance bands, demonstrating that the algal extract active group capping of nanoparticles is what makes them more stable and effective (Ismail et al., 2021).

In the present study, Fig. 1a and b show TEM imaging of USeNPs with a smooth spherical shape and particle size ranging from 46.03 to 83.80nm, whereas Figure 2 shows SEM imaging of USeNPs with an oval, spherical form and particle size ranging from (24.32 - 27.53) nm. Figures 3 and 4 show the EDX examination of the selenium elemental composition of USeNPs, which contained 1.55 atomic % and 8.31 mass %, validating the creation of USeNPs. In addition, the other EDX peaks detected included K, C, N, P, S, Si, Mg, Ca, and O, with 0.16 ± 0.02, 43.96 ± 0.25, 14.80 ± 0.41, 0.60 ± 0.04, 0.87 ± 0.04, 0.18± 0.03, 0.58 ± 0.04, 0.59 ± 0.04, and 29.95 ± 0.43 mass %, respectively, and 0.06 ± 0.01, 53.91 ± 0.31, 15.56 ± 0.43, 0.29 ± 0.02, 0.40 ± 0.02, 0.09± 0.01, 0.35 ± 0.02, 0.22 ± 0.01 and 27.57 ± 0.40 atom % respectively.

In vitro, assays are one of the main methodologies used in cell migration research since they allow researchers to quantify cell migration capacity quantitatively under controlled experimental settings (Kramer et al., 2013; Grada et al., 2017). The scratch test is ideal for studying cell migration since it is inexpensive and straightforward (Liang et al., 2007; Kramer et al., 2013).

In scratch tests, multiple quantification approaches are employed to quantify collective cell migration (Topman et al., 2012). To test the cytotoxicity of USeNPs, we measured the change in gap width using WISH cells (Masuzzo et al., 2016; Grada et al., 2017). We computed the wound width at zero time and after 24h, as well as the healing percentage. Figure 5A-C depicts cell migration and wound healing by calculating the change in gap size (µm) as a function of time; the initial gap size was found to be 2424003µm, and after 24 h was 612700 and 429700µm, with 74.72% and 82.27% healing for control and USeNPs (500µg/mL) treated cells, respectively. WISH cells with IC_{50}= 904.8µg/mL (Table 1) achieved 66% viability and 34% inhibition at the used USeNPs concentration (500µg/mL), demonstrating no risk of utilizing USeNPs in wound healing.

Boomi et al. (2020) investigated the wound healing capacity of phyto-engineered gold nanoparticles and proposed that this capacity leads to faster skin regeneration, which promotes wound healing in the presence of gold nanoparticles. Zhang et al. (2022) also reported that selenium nanoparticles have a promising effect on curcumin-incorporated nanofiber matrices in fibroblast cell adhesion and proliferation, which promotes wound healing in tumor-bearing mice during tumor therapies as suggested by Meng et al. (2022).

The anti-inflammatory activity of UseNPs was determined by evaluating their inhibitory effect on the Cox-1 enzyme, lowering oxidative stress, and alleviating gout and arthritic pain. Cox enzyme performed the key initial step in the arachidonic acid metabolic cascade, resulting in the synthesis of pro-inflammatory prostaglandins, thromboxanes, and prostacyclins. Prostaglandins regulate smooth muscle contractility, blood pressure, and platelet aggregation, and mediate fever and discomfort. Many nonsteroidal anti-inflammatory medications work by inhibiting cyclooxygenase activity to produce analgesic, antipyretic, anti-inflammatory, and antithrombotic effects (Lee et al., 2003).

Maintenance of physiological proteinoid biosynthesis is the role of Cox-1. Figure 6 depicts the inhibitory effect of USeNPs relative to the reference standard indomethacin, which inhibits the (Cox-1) enzyme. USeNPs inhibited Cox-1 activity at all concentrations except concentrations (0.25-0.5-1) µg/mL, where no inhibition was observed for the Cox-1 enzyme. The highest concentration of USeNPs (500µg/mL) exhibited the maximum inhibition (69.41%) with IC_{50} = 215.01µg/mL but did not surpass the reference indomethacin.

SeNPs of *U. lactuca* have a remarkable antifungal effect on *C. neoformas* RCMB

0049001 and *C. lipolytica* RCMB 005007(1), as evidenced by a robust inhibition zone measuring 9.667 mm and 8.8333 mm, respectively. While no effect on *G. candidum* RCMB 041001 was detected. In contrast, the antibiotic ketoconazole did not inhibit the proliferation of any tested fungal pathogens (Table 2). Lotfali et al. (2021) found that silver and selenium nanoparticles exhibited promising antifungal activity against various *Candida* species and *C. neoformans*. They also illustrated the nanoparticle's inhibitory effect on resistant isolates, which included interference with the cell wall synthesis and inhibition of ergosterol synthesis (Lotfali et al., 2021). These findings supported our results.

USeNPs MIC on fungal tested strains was calculated as shown in Table 3. Concentration 78.1µg/mL showed promising inhibition against *C. neoformas* RCMB 0049001, while concentration 312.5µg/mL showed significant inhibition against *C. lipolytica* RCMB 005007(1). The synthesized USeNPs had superior antifungal activity against *C. neoformas* RCMB 0049001 compared to *C. lipolytica* RCMB 005007(1).

While Lotfali et al. (2021) discovered that silver nanoparticles showed antifungal action against *Candida glabrata* when compared to selenium nanoparticles, while no inhibition occurred in the range of 0.125g/mL (low concentration); 0.125g/mL or higher decreased growth compared to the control. According to our MIC data, USeNPs exhibited potential antifungal capabilities, making them a viable alternative to drug-resistant isolates. According to Vijayakumar et al. (2013), the positive charge of silver ions is responsible for their antibacterial activity via electrostatic interactions with negatively charged microbes' cell membranes (Vijayakumar et al., 2013), which may also be said for our USeNPs in the current study.

The combination of USeNPs and ketoconazole inhibited *C. neoformas* RCMB 0049001, followed by *C. lipolytica* RCMB 005007(1), with inhibition zones of 12.83, 10.173, respectively, when using the treatment formula of 2.5mg/mL USeNPs mixed with ketoconazole 100µg/mL. This increase in ketoconazole activity was most likely achieved by increasing USeNps concentrations to 5mg/mL, which can result in a larger inhibition zone diameter; 15.25, 14.167, respectively, against *C. neoformas* RCMB 0049001, followed by *C. lipolytica* RCMB 005007(1).

According to our findings, ketoconazole alone cannot inhibit fungal growth, but when combined with our USeNPs, the inhibition effect was significantly increased, which is deemed a novel, fascinating, and appealing conclusion that intends to strengthen the ketoconazole effect on fungi. However, the mechanism of synergistic activity is still unknown. Our findings revealed a promising synergistic impact against *C. neoformas* RCMB 0049001 when USeNPs were combined with ketoconazole, as shown in Table 4 and clearly in Fig. 7. El-Deeb et al. (2018) earlier indicated that nanoparticles increase antibiotic reaction rates in a synergistic manner and on diverse types of bacteria (El-Deeb et al., 2018). The enhancement of antibiotic, antimicrobial activity with selenium nanoparticles may be due to the reaction that bonds antibiotics and nanoparticles, then the antibiotic-selenium nanoparticle may attach to the pathogen cell membrane, resulting in cell wall lysis, followed by SeNPs-antibiotic combination entrance into the pathogen cell, which may result in DNA unwinding, leading to cell death, as suggested by Krishna et al. (2015).

In the case of bacterial pathogens, Huang et al. (2016) developed antibacterial selenium nanoparticles agents (quercetin-acetylcholine-SeNPs) with great stability and outstanding antibacterial and bactericidal properties against pathogenic microorganisms (Huang et al., 2016). This product can combine with the acetylcholine receptor that occurs on the bacterial cell membrane due to acetylcholine presence, which increases cell membrane permeability, which causes pathogen membrane disruption and cytoplasm leakage, allowing nanoparticles to invade bacterial cells and disrupt DNA structure. This demonstrated that combining antibiotics and selenium nanoparticles could improve antibiotic efficacy against resistant microorganisms.

The TEM data from the current study provided a more complete image and a deeper understanding of cellular morphological degenerations. The TEM micrographs of *C. neoformas* RCMB 0049001 treated with USeNPs individually and in combination with ketoconazole are shown in Fig. 8A-F. Micrographs of individual *C. neoformas* RCMB 0049001cells in the control sample revealed only spherical or oval-cylindrical

shaped conidia (Fig. 8A, B). Figures 8C and D show yeast cells with aberrant shapes, some holes, and deformed membranes after treatment with USeNPs in *C. neoformas* RCMB 0049001. Figure 8 E, F illustrated that after treatment with USeNPs in combination with the antifungal ketoconazole, the cell membrane has atypical surface bulges and has lost its smoothness, resulting in cell membrane breakdown. Our TEM images were supported by Lotfali et al.'s (2021) findings, which revealed that when *C. glabrata* was treated with silver nanoparticles, this yeast developed holes and aberrant morphology. USeNPs displayed strong antifungal efficacy against resistant *C. neoformans* strains in our investigation, which could be due to full membrane breakdown, hole formation, and, finally, cell death; this condition was also supported by Lotfali et al. (2021). It is also worth mentioning that Lotfali et al. (2021) proposed that treating *C. glabrata* with silver and selenium nanoparticles resulted in the loss of DNA replication ability, ribosomal subunit protein production, and critical enzymes, all of which resulted in the inactivation of microorganisms.

The dramatic changes in *Cryptococcus* cell structure depicted in the transmission micrographs were consistent with the mode of action described by Hu et al. (2017), who stated that the action of ketoconazole as an antifungal agent is accomplished by inhibiting the cytochrome P450 14-demethylase enzyme. At the same time this enzyme reduces fungal triglyceride and phospholipid manufacture, and this antibiotic also inhibits lanosterol synthesis, a key precursor for ergosterol biosynthesis. Ergosterol is critical for the integrity of fungal membranes. Fungal membrane fluidity is caused by ergosterol leakage, which inhibits fungal growth (Hu et al., 2017).

Kim et al. (2008) investigated the inhibitory activity of silver nanoparticles on the growth of several harmful fungi, including *Trichophyton* and *Microsporum* spp. According to our findings, USeNPs showed a potential antifungal effect and could be employed as a medication for drug-resistant isolates.

Conclusion

In conclusion, the synthesized USeNPs demonstrated significantly enhanced ketoconazole antifungal activity against resistant pathogenic fungal yeast strains via the fungal cell membrane and wall structure modifying resistance strains. Finally, we demonstrated the wound healing capacity of USeNPs *in vitro* by assessing their anti-inflammatory activity against the Cox1 enzyme as well as their fungicidal powers against ketoconazole-resistant *C. neoformans* and *C. lipolytica* strains. This could be advantageous in the application of USeNPs in wound treatment and could be expanded further to textile technology.

We also suggested encapsulating antifungal drugs in combination with the mentioned nanoparticles to reduce side effects and increase drug effectiveness. This prompted us to include USeNPs (alone or combined with ketoconazole) in the medicinal protocols treating severe infections caused by pathogenic yeast cells. Following specific medical trials, their synergistic results support their promise as a safe therapy for severe fungal and *Candida* infections, as well as a good anti-inflammatory medicine.

Acknowledgement: The authors thank Dr Kay Howard of Murdoch University, Western Australia, 6150, Australia for checking the English expression before manuscript submission.

Competing interests: The authors report no conflicts of interest regarding this work.

Authors contributions': Conceptualization, M.M.E., M.E.M.M., K.El-T; methodology, M.E.M.M, and A.E.; software, M.E.M.M, and A.E.; validation, M.M.E., and M.E.M.M.; formal analysis, M.E.M.M.; investigation, A.E.; resources, M.E.M.M, M.M.A., and A.E.; data curation, M.E.M.M, and A.E.; writing—original draft preparation, M.E.M.M, A.E., and K.El-T; writing—review and editing, M.M.E., MMA., and K. El-T; visualization, M.M.E.; project administration, M.M.E.; All authors have read and agreed to the published version of the manuscript.

Ethics approval: Not applicable.

Funding: This research received no internal or external funding.

References

Aabed, K., Mohammed, A.E. (2021) Synergistic and antagonistic effects of biogenic silver nanoparticles in combination with antibiotics

against some pathogenic microbes. *Frontiers in Bioengineering and Biotechnology*, **9**, 652362. doi:10.3389/fbioe.2021.652362

Abdel-Aziz, A.A., El-Azab, A.S., Abou-Zeid, L.A., ElTahir, K.E., Abdel-Aziz, N.I., Ayyad, R.R., Al-Obaid, A.M. (2016) Synthesis, anti-inflammatory, analgesic and COX-1/2 inhibition activities of anilides based on 5,5-diphenylimidazolidine-2,4-dione scaffold: Molecular docking studies. *European Journal of Medical Chem*istry, **115**, 121-131.

Abdel-Moneim, A.E., El-Saadony, M.T., Shehata, A.M., Saad, A.M., Aldhumri, S.A., Ouda, S.M., Mesalam, N.M. (2022) Antioxidant and antimicrobial activities of *Spirulina platensis* extracts and biogenic selenium nanoparticles against selected pathogenic bacteria and fungi. *Saudi Journal of Biological Sciences*, **29**, 1197–1209.

Abo-Neima, S.E., Ahmed, A.A., El-Sheekh, M., Makhlof, M.E.M. (2023) *Polycladia myrica*-based delivery of selenium nanoparticles in combination with radiotherapy induces potent *in vitro* antiviral and *in vivo* anticancer activities against Ehrlich ascites tumor. *Frontiers in Molecular Biosciences*, **10**, 1120422. doi:10.3389/fmolb.2023.1120422

Amin, B.H. (2016) Isolation and characterization of antiprotozoal and antimicrobial metabolite from *Penicillium roqueforti*. *African Journal of Mycology and Biotech*nology, **21**, 13-26.

Amin, B.H., Abou-Dobara, M.I., Diab, M.A., Gomaa, E.A., El-Mogazy, M.A., El-Sonbati, A.Z., EL-Ghareib, M.S., Hussien, M.A. Salama, H.M., (2020) Synthesis, characterization, and biological investigation of new mixed-ligand complexes. *Applied Organometallic Chemistry,* **34**, 5689. doi:10.1002/aoc.5689

Amin, B.H., Amer, A., Azzam, M., Abd El-Sattar, N.E.A., Mahmoud, D., Al-Ashaal, S., Al-Khalaf, A.A., Hozzein, W. N. (2022) Antimicrobial and anticancer activities of *Periplaneta americana* tissue lysate: An *in vitro* study. *Journal of King Saud University of Sci*ences, **34**, 102095. doi:10.1016/j.jksus.2022.102095

Amin, H.H. (2019) *Ulva lactuca* as a cheap and safe bio pesticide in fields and its chemical composition (*in vitro*). *Egyptian Journal of Aquatic Biology and Fisheries*, **23**, 415-428.

Amin, H.H. (2020) Biosynthesized silver nanoparticles using *Ulva lactuca* as a safe synthetic pesticide (*in vitro*). *Open Agric*ulture, **5,** 291-299.

Araújo, G.R.S., Alcantara, C.L., Rodrigues, N., de Souza, W., Pontes, B., Frases, S. (2021) Ultrastructural Study of *Cryptococcus neoformans* Surface During Budding Events. *Frontiers in Microbiology,* **12**, 609244. doi:10.3389/fmicb.2021.609244

Blanco-Fernandez, B., Castaño, O., Mateos-Timoneda, M.Á., Engel, E., Pérez-Amodio, S. (2021) Nanotechnology approaches in chronic wound healing. *Advances in Wound Care,* **10,** 234-256.

Boomi, P., Ganesan, R., Prabu Poorani, G., Jegatheeswaran, S., Balakumar, C., et al. (2020) Phyto-Engineered gold nanoparticles (aunps) with potential antibacterial, antioxidant, and wound healing activities under *in vitro* and *in vivo* conditions. *International Journal of Nanomedicine,* **15**, 7553-7568.

Chugh, D., Viswamalya, V.S., Das, B. (2021) Green synthesis of silver nanoparticles with algae and the importance of capping agents in the process. *Journal of Genetic Engineering and Biotechnol*ogy, **19,** 126. doi:10.1186/s43141-021-00228-w

Eldarier, S.M., Abou-Zeid, H.M., Marzouk, R.I., Abo Hatab, A.S. (2020) Biosynthesis of silver nanoparticles via *Haplophyllum tuberculatum* (Forssk.) A. Juss.(Rutaceae) and its use as bioherbicide. *Egyptian Journal of Botany,* **60**(1), 25-40.

El-Deeb, B., Al-Talhi, A., Mostafa, N., Abou-assy, R. (2018) Biological synthesis and structural characterization of selenium nanoparticles and assessment of their antimicrobial properties. *American Scientific Research Journal for Engineering, Technology, and Sciences,* **45**, 135-170.

Ellis, D., Watson, A. (1996) Systemic antifungal agents for cutaneous fungal infections. *Australian Prescriber,* **19**, 72-5.

El Maghraby, D., Hassan I. (2021) Photosynthetic and

biochemical response of *Ulva lactuca* to marine pollution by polyaromatic hydrocarbons (PAHs) collected from different regions in Alexandria City, Egypt. *Egyptian Journal of Botany,* **61**(2), 467-478.

EL-Saadony, M.T., Abd El-Hack M.E., Swelum, A.A., Al-Sultan, S.I., EL-Ghareeb, W.R., Hussein, E.O., et al. (2021) Enhancing quality and safety of raw buffalo meat using the bioactive peptides of pea and red kidney bean under refrigeration conditions. *Italian Journal Animal Sci*ences, **20**, 762-776.

Elsayed, A., El-Shamy, G.M., Attia, A.A. (2022) Biosynthesis, characterization, and assessment of zirconia nanoparticles by *Fusarium oxysporum* species as potential novel antimicrobial and cytotoxic agents. *Egyptian Journal of Botany,* **62**(2), 507-522.

El-Sheekh, M.M., Hassan, L.H., Morsi, H.H. (2021) Assessment of the *in vitro* anticancer activities of cyanobacteria mediated silver oxide and gold nanoparticles in human colon CaCo-2 and cervical HeLa cells. *Environmental Nanotechnology,* **16**, 100556. doi:10.1016/J.ENMM.2021.100556.

Ericsson, H.M., Sherris, J.C. (1971) Antibiotic sensitivity testing. Report of an international collaborative study. *Acta Pathologica et Microbiologica Scandinavica. Section B, Microbiology and Immunology,* **11**, 217.

Grada, A., Otero-Vinas, M., Prieto-Castrillo, F., Obagi, Z., Falanga, V. (2017) Research techniques made simple: analysis of collective cell migration using the wound healing assay. *Journal of Investigative Dermatology,* **137**, 11– 16.

Haudenschild, C.C., Schwartz, S.M. (1979) Endothelial regeneration. II. Restitution of endothelial continuity. *Laboratory Investigation,* **41**, 407-18.

Hifney, A.F, Soliman, Z., Ali, E.F., Hussein, N.A. (2022) Microbial and microscopic investigations to assess the susceptibility of *Candida parapsilosis* and *Prototheca ciferrii* to phyco-synthesized titanium dioxide nanoparticles and antimicrobial drugs. *South African Journal of Botany*,**151**, 791-799.

Hu, Z., He B., Ma L., Sun Y., Niu Y., Zeng, B. (2017) Recent advances in ergosterol biosynthesis and regulation mechanisms in *Saccharomyces cerevisiae*. *Indian Journal of Microbiol*ogy, **57**, 270-277.

Huang, X., Chen, X., Chen, Q, Yu, Q., Sun, D., Liu, J. (2016) Investigation of functional selenium nanoparticles as potent antimicrobial agents against superbugs, *Acta Biomaterialia,* **30**, 397-407.

Ismail, G.A., El-Sheekh, M.M., Samy, R.M., Gheda, S.F. (2021) Antimicrobial, antioxidant and antiviral activities of biosynthesized silver nanoparticles by phycobiliproteins crude extract of the cyanobacteria *Spirulina platensis* and *Nostoc linckia*. *Bionanoscience,* **11**, 355–370.

Jacob, J.M., Ravindran, R., Narayanan, M., Samuel, S.M., Pugazhendhi, A., Kumar, G. (2021) Microalgae: a prospective low-cost green alternative for nanoparticle synthesis. *Current Opinion in Environmental Science and Health,* **20**, 100–163.

Jain, A. (2022) Algae-mediated synthesis of biogenic nanoparticles. *Advances in Natural Sciences: Nanoscience and Nanotechnology*, **13**, 043001. doi:10.1088/2043-6262/ac996a

Kim, K.J., Sung, W.S., Moon, S.K., Choi, J.S., Kim, J.G., Lee, D.G. (2008) Antifungal effect of silver nanoparticles on dermatophytes. *Journal of Microbiology and Biotechnol*ogy, **18**, 1482-1484.

Kramer, N., Walzl, A., Unger, C., Rosner, M., Krupitza, G., Hengstschläger, M., Dolznig, H. (2013) *In vitro* cell migration and invasion assays. *Mutation Research,* **752**, 10–24.

Krishna, G., Kumar, S.S., Pranitha, V., Alha, M, Charaya, S. (2015) Biogenic synthesis of silver nanoparticles and their synergistic effect with antibiotics: A study against *Salmonella* sp. *International Journal Pharmacy and Pharmaceutical Sciences*, **7**, 84-88.

Kumar, D., Lundgren, D.W., Moore, R.M., Silver, R.J., Moore, J.J. (2004) Hydrogen peroxide induced apoptosis in amnion-derived wish cells is not inhibited by vitamin C. *Placenta,* **25**, 266-272.

Lee, J.L., Mukhtar, H., Bickers, D.R., Kopelovich, L., Athar, M. (2003) Cyclooxygenases in the skin:

pharmacological and toxicological implications. *Toxicology and Applied Pharmacology,* **192**, 294-306.

Liang, C.C., Park, A.Y., Guan, J.L. (2007) *In vitro* scratch assay: a convenient and inexpensive method for analysis of cell migration *in vitro*. *Natural Protocols,* **2**, 329–333.

Liao, T.L., Chen, Y.M., Chen, D.Y. (2016) Risk factors for cryptococcal infection among patients with rheumatoid arthritis receiving different immunosuppressive medications. *Clinical Microbiology and Infection,* **22**, 815.e1-815. doi:10.1016/j.cmi.2016.05.030

Lotfali, E., Toreyhi, H., Sharabiani, K.M., Fattahi, A., Soheili, A., Ghasemi, R., Keymaram M., Rezaee, Y., Iranpanah, S. (2021) Comparison of antifungal properties of gold, silver, and selenium nanoparticles against amphotericin b-resistant *Candida glabrata* clinical isolates. *Avicenna Journal Medical Biotechnol*ogy, **13**, 47-50.

Makhlof, M.E.M., Albalwe, F.M., Al-Shaikh, T.M., El-Sheekh, M.M. (2022) Suppression effect of *Ulva lactuca* selenium nanoparticles (USeNPs) on HepG2 carcinoma cells resulting from degradation of epidermal growth factor receptor (EGFR) with an evaluation of its antiviral and antioxidant activities. *Applied Sciences*, **12**, 11645. doi:10.3390/app122211546

Masuzzo, P., Van Troys, M., Ampe, C., Martens, L. (2016) Taking aim at moving targets in computational cell migration. *Trends Cell Biology,* **26**, 88–110.

McFadden, D., Zaragoza, O., Casadevall, A. (2006) The capsular dynamics of *Cryptococcus neoformans. Trends in Microbiology* **14**, 497-505.

Mohamed, R.M., Fawzy, E.M., Shehab, R.A., Abdel-Salam, M.O., Salah El Din, R.A., Abd El Fatah, H.M. (2022) Production, characterization, and cytotoxicity effects of silver nanoparticles from brown alga (*Cystoseira myrica*). *Journal Nanotechnol*ogy, **2022**, 6469090. doi:10.1155/2022/6469090

Naskar, A., Kim, K.S. (2020) Recent advances in nanomaterial-based wound-healing therapeutics. *Pharmaceutics,* **12**, 499. doi:10.3390/pharmaceutics12060499

Perfect, J.R. (2013) Fungal diagnosis: how do we do it and can we do better? *Current Medical Research and Opin*ion, **29**, 3-11.

Rajasingham, R., Smith, R.M., Park, B.J., Jarvis, J.N., Govender, N.P., Chiller, T.M., Denning, D.W., Loyse, A., Boulware, D.R. (2017) Global burden of disease of HIV-associated cryptococcal meningitis: an updated analysis. *Lancet Infectious Diseases*, **17**, 873-881.

Rónavári, A., Igaz, N., Gopisetty, M.K., Szerencsés, B., Kovács, D., Papp, C., et al. (2018) Biosynthesized silver and gold nanoparticles are potent antimycotics against opportunistic pathogenic yeasts and dermatophytes. *International Journal of Nanomedicine*, **13**, 695-703.

Sampath, S., Madhavan, Y., Muralidharan, M., Sunderam, V., Lawrance, A.V., Muthupandian, S. (2022) A review on algal mediated synthesis of metal and metal oxide nanoparticles and their emerging biomedical potential. *Journal of Biotechnol*ogy, **360**, 92-109.

Saquib, Q., Al-Khedhairy, A.A., Siddiqui, M.A., Abou-Tarboush, F.M., Azam, A., Musarrat, J. (2012) Titanium dioxide nanoparticles induced cytotoxicity, oxidative stress and DNA damage in human amnion epithelial (WISH) cells. *Toxicology in Vitro,* **26**, 351-61.

Shalaby, M.A., Anwar, M.M., Saeed, H. (2022) Nanomaterials for application in wound Healing: current state-of-the-art and future perspectives. *Journal of Polymer Res*earch, **29**, 91. doi:10.1007/s10965-021-02870-x

Toczek, J., Sadłocha, M., Major, K., Stojko, R. (2022) Benefit of silver and gold nanoparticles in wound healing process after endometrial cancer protocol. *Biomedicines,* **10**, 679. doi: 10.3390/biomedicines10030679

Todaro, G.J., Lazar, G.K., Green, H. (1965) The initiation of cell division in a contact-inhibited mammalian cell line. *Journal of Cellular and Comparative Physiology,* **66**, 325-33.

Topman, G., Sharabani-Yosef, O., Gefen, A. (2012) A standardized objective method for continuously measuring the kinematics of cultures covering a mechanically damaged site. *Medical Engineering and Physics,* **34**, 225-32.

Touliabah, H.E., EL-Sheekh, M.M., Makhlof, M.E.M (2022) Evaluation of *Polycladia myrica* mediated selenium nanoparticles (CsSeNPS) cytotoxicity against PC-3 cells and antiviral activity against HAV HM175 (Hepatitis A), HSV-2 (Herpes simplex II) and Adenovirus strain 2. *Frontiers in Marine Sciences,* **9**, 1092343. doi:10.3389/fmars.2022.1092343

Verma, A.K., Kumar, P. (2022) On recent developments in biosynthesis and application of au and ag nanoparticles from biological systems. *Journal of Nanotechnol*ogy, **2**, doi:10.1155/2022/5560244

Vijayakumar, M., Priya, K., Nancy, F.T., Noorlidah, A., Ahmed, A.B.A. (2013) Biosynthesis, characterisation and anti-bacterial effect of plant-mediated silver nanoparticles using *Artemisia nilagirica*. *Industrial Crops and Prod*ucts, **41**, 235-40.

World Health Organization (WHO) (2018) Guidelines for The Diagnosis, Prevention and Management of Cryptococcal Disease in HIV-Infected Adults, Adolescents and Children: Supplement to the 2016 Consolidated Guidelines on the Use of Antiretroviral Drugs for Treating and Preventing HIV Infection. https://apps.who.int/iris/handle/10665/260399

Yedurkar, S.M., Maurya, C.B., Mahanwar, P.A. (2017) A biological approach for the synthesis of copper oxide nanoparticles by *Ixora coccinea* leaf extract. *Journal of Materials and Environmental Sciences,* **8**, 1173-1178.

Youssef, G.A., El-Boraey, A.M., Abdel-Tawab, M.M. (2019) Eco-friendly green synthesis of silver nanoparticles from Egyptian honey: evaluating its antibacterial activities. *Egyptian Journal of Botany,* **59**(3), 709-721.

Zhang, M., Zhang, J., Ran, S., Sun, W., Zhu, Z. (2022) Polydopamine-assisted decoration of Se nanoparticles on curcumin-incorporated nanofiber matrices for localized synergistic tumor-wound therapy. *Biomaterials Sciences*, **10**, 536-548.

التقييم في المختبر لجسيمات السيلينيوم النانوية بواسطة جزيئات نانو السيلينيوم من طحلب الاولفا لاكتوكا من خلال رفع تأثير المضاد الحيوي الكيتوكونازول ضد أنواع من الخمائر الممرضة وقدرة التئام الجروح من خلال تثبيط نشاط انزيمات الأكسدة الحلقية

مفيدة مخلوف[1]، مصطفي الشيخ[2]، ماجدة التويجري[3]، خالد الطرابيلي[4]، عبير السيد[1]

[1] قسم النبات والميكروبيولوجي- كلية العلوم- جامعة دمنهور- دمنهور- مصر، [2] قسم النبات – كلية العلوم- جامعة طنطا- طنطا - مصر، [3] قسم البيولوجي- كلية العلوم التطبيقية- جامعة أم القري- مكة المكرمة- المملكة العربية السعودية، [4] قسم علوم الحياة- كلية العلوم جامعة الامارات العربية المتحدة- العين - الامارات العربية المتحدة.

تم تصنيع وتوصيف جزيئات السيلينيوم النانوية لطحلب الاولفا لاكتوكا. ثم فحصت قدرتها على التئام الجروح من خلال اختبار في المختبر يظهر شفاء واعدًا بنسبة 82.27٪ بتركيز 500 ميكروجرام/ملي. تم تحديد الإمكانات المضادة للفطريات عبر تقنية انتشار آجار اجار، والتركيز المثبط الأدنى. والذي تم تقييمه بواسطة مقايسة التخفيف الدقيق. تمت دراسة التأثير

تمت دراسة التأثير التآزري لجزيئات السيلينيوم النانوية بشكل فردي أو بالاشتراك مع المضادات الحيوية القياسية المضادة للفطريات (الكيتوكونازول، 100 ميكروغرام/ مل) ضد كريبتوكوكس نيوفورمانس وكانديدا ليبوليتكا. تم فحص جيوتريكيم كانديديم بواسطة مقايسة انتشار آجار آجار، متبوعًا بالمجهر الإلكتروني الثاقب لتقييم التغييرات المختلفة في خلايا الخميرة الفطرية الأكثر حساسية. أشارت النتائج إلى أن جزيئات السيلينيوم النانوية لطحلب الاولفا لاكتوكا لها تأثير واعد ضد كريبتوكوكس نيوفورمانس وكانديدا ليبوليتكا من خلال تحقيق مناطق تثبيط ملحوظة. بالمقارنة ، لم يتم الكشف عن أي تأثير على جيوتريكيم كانديديم .تتميزجزيئات السيلينيوم النانوية لطحلب الاولفا لاكتوك الاصطناعية حيويًا بإمكانيات قوية مضادة للفطريات ويمكن أن ترفع وتقوي من تأثير المضاد الحيوي الكيتوكونازول تجاه مسببات الأمراض الفطرية المختلفة ، وكان هذا واضحًا في التجربة التآزرية التي أجريت في هذه الدراسة على أساس الجمع بين الكيتوكونازول ؛ 100 ميكروغرام / مل مع جزيئات السيلينيوم النانوية مما ادي الي انفصال في خلايا كريبتوكوكس نيوفورمانس مع تغيير جذري حاد.